



**HAL**  
open science

## Multiyear validation of the NRL-G2S wind fields using infrasound from Yasur

K Antier, A. Le Pichon, S Vergniolle, C Zielinski, M Lardy

► **To cite this version:**

K Antier, A. Le Pichon, S Vergniolle, C Zielinski, M Lardy. Multiyear validation of the NRL-G2S wind fields using infrasound from Yasur. *Journal of Geophysical Research: Atmospheres*, 2007, 10.1029/2007JD008462 . insu-01288749

**HAL Id: insu-01288749**

**<https://insu.hal.science/insu-01288749>**

Submitted on 15 Mar 2016

**HAL** is a multi-disciplinary open access archive for the deposit and dissemination of scientific research documents, whether they are published or not. The documents may come from teaching and research institutions in France or abroad, or from public or private research centers.

L'archive ouverte pluridisciplinaire **HAL**, est destinée au dépôt et à la diffusion de documents scientifiques de niveau recherche, publiés ou non, émanant des établissements d'enseignement et de recherche français ou étrangers, des laboratoires publics ou privés.

## Multiyear validation of the NRL-G2S wind fields using infrasound from Yasur

K. Antier,<sup>1</sup> A. Le Pichon,<sup>1</sup> S. Vergnolle,<sup>2</sup> C. Zielinski,<sup>2</sup> and M. Lardy<sup>3</sup>

Received 26 January 2007; revised 26 April 2007; accepted 14 September 2007; published 15 December 2007.

[1] The Yasur volcano in the Vanuatu archipelago is an outstanding source of infrasonic waves due to its regular activity. This volcano is permanently monitored by the IS22 infrasound station located in New Caledonia, about 400 km from it, and by one microbarometer installed close to its crater. A multiyear monitoring of Yasur is proposed to validate consistently the Naval Research Laboratory Ground to Space (NRL-G2S) semiempirical atmospheric model up to the stratosphere. The results of propagation modeling accurately explain seasonal changes as well as small short-timescale variations of the infrasonic observables. The azimuthal deviation is predicted with an uncertainty in general lower than  $0.5^\circ$ . The fluctuations of the trace velocity and the celerity are simulated with errors as large as 5 m/s. This study demonstrates that the use of appropriate propagation tools along with the NRL-G2S specifications provides accurate enough results for most of the long-range observations for the purpose of operational infrasound monitoring.

**Citation:** Antier, K., A. Le Pichon, S. Vergnolle, C. Zielinski, and M. Lardy (2007), Multiyear validation of the NRL-G2S wind fields using infrasound from Yasur, *J. Geophys. Res.*, 112, D23110, doi:10.1029/2007JD008462.

### 1. Introduction

[2] Infrasonic waves propagate in the atmosphere over very large distances in the waveguide formed by the atmosphere, its temperature gradients and its wind speed variations. Ducting is especially efficient in the ground to stratosphere and thermosphere waveguides. It can be reinforced or reduced by the high altitude winds [Kulichkov *et al.*, 2004; Garcés *et al.*, 2004]. As acoustic waves propagate in the upper atmosphere, the wavefront characteristics reveal, in addition to information about the source, significant features of the vertical structure of the winds. The interpretation of these data motivated studies on sources of infrasonic waves and their propagation in the upper atmosphere.

[3] Infrasonic waves from naturally occurring geophysical phenomena have been observed since early in the last century. The interpretation of these data motivated studies on their propagation in the upper atmosphere [Donn and Rind, 1971; Rind, 1978]. However, results were mainly qualitative. Taking advantage of new signal processing methods and efficient array design, measurements of permanent sources of infrasound are now available and provide a basis for more accurate atmospheric investigations [Bush *et al.*, 1989; Hedlin *et al.*, 2002].

[4] As repetitive ground truth events, volcanic eruptions are very valuable for atmospheric studies [Wilson and Forbes, 1969; Liszka and Garcés, 2002; Olson *et al.*, 2006; Wilson *et*

*al.*, 2006]. The equivalent yield of explosive eruptions varies from a small fraction of a Kiloton of TNT, for many eruptions, up to a few Megatons for rare events such as the Mount St. Helens eruption (USA, 1980) [Donn and Balachandran, 1981; Reed, 1987; Delclos *et al.*, 1990]. Basaltic eruptions also produce sound waves during Strombolian explosions [Ripepe *et al.*, 1996; Vergnolle and Brandeis, 1996].

[5] The main objective of this paper is to demonstrate the capability of measuring small temporal wind fluctuations from the ground to the stratosphere, thanks to a continuous monitoring of active volcanoes. We first present the experimental setting in the Vanuatu region for the monitoring of one active volcano permanently generating infrasound signals. Then, by comparing observations to simulation results over several years, we estimate errors in the predicted infrasound observables. Finally, we discuss the validity of the upper-wind model used in our simulations for the purpose of operational infrasound monitoring.

### 2. Listening to Yasur in the Near and Far Field

[6] The Vanuatu archipelago, located in the South Pacific between New Caledonia and Fiji, is composed by more than 80 islands and islets. Although the large majority of volcanoes in that tectonic context produce an explosive activity with silicic magmas, those emitted around Vanuatu are largely basaltic, but more viscous, allowing explosions at their vents [Robin and Monzier, 1994; Lardy *et al.*, 1999].

[7] The implementation of the International Monitoring System (IMS) for the monitoring of the Comprehensive Test Ban Treaty (CTBT) increases the need to identify and analyze geophysical events [Hedlin *et al.*, 2002]. The IS22 infrasound array (New Caledonia,  $22.19^\circ\text{S}$ ;  $166.84^\circ\text{E}$ ) is part of the

<sup>1</sup>CEA/DASE/LDG, Bruyères-le-Châtel, France.

<sup>2</sup>LDSG-IPGP, Paris, France.

<sup>3</sup>IRD Center, Nouméa, New Caledonia.

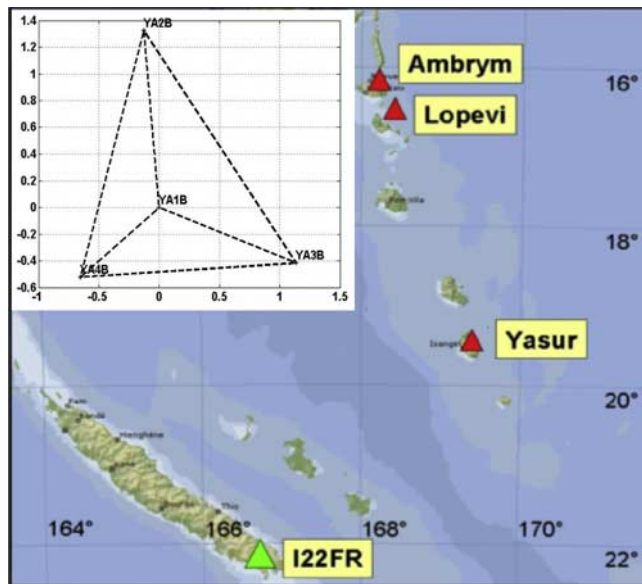


**Figure 1.** Geographic context of the Archipelago of Vanuatu in Oceania. The green triangle indicates the location of the IS22 infrasound station (New Caledonia). The red triangles indicate the active volcanoes permanently detected by this station (map source: Microsoft Encarta). Yasur is located at 399 km to the north-northeast ( $42.7^\circ$  clockwise from north) of IS22. The inset shows the relative positions of the four MB2000-type microbarometers composing the IS22 array (the x and y scales are in kilometers).

global infrasonic network of the IMS. It consists of four MB2000-type microbarometers, 1 to 3 km apart. The MB2000 has been designed to operate from DC up to 27 Hz with an electronic noise level of 2 mPa RMS in the 0.02–4 Hz frequency band. Among other signals of natural origin, the array continuously detects coherent infrasonic waves originating from three active volcanoes (Figure 1) [Le Pichon *et al.*, 2005a, 2005b]. The nearest one, Yasur ( $19.52^\circ\text{S}$ ,  $169.42^\circ\text{E}$ , 360 meters high), is producing a series of explosions, whose characteristics vary between Strombolian and mild-Vulcanian [McClelland *et al.*, 1989]. These are triggered by the sudden decompression of the inner magmatic gas, which expels magma fragments at the vent with large velocities. Its regular activity (several hundred explosions per day are generally measured during particularly active periods), combined with its accessibility, make of it one of the most studied volcano (geological, seismic and thermal surveys). The wave parameters of the infrasonic waves, such as back-azimuth, trace velocity and central frequency, are calculated with the PMCC method (Progressive Multi-Channel Correlation) [Cansi, 1995]. This correlation-based method, originally designed for seismic arrays, proved to be very efficient for infrasonic data and is well adapted for analyzing low-amplitude coherent waves within non-coherent noise.

[8] Due to the low particle density and non-linear dissipation in the upper atmosphere, thermospheric returns are strongly attenuated at a range of hundreds of kilometers with absorption increasing with frequency [Bass and Sutherland, 2004]. Considering the relative high frequency

content (from 1 to 5 Hz, depending on the crisis) of the signals from Yasur (Figure 2), thermospheric arrivals are thus unlikely and most of the acoustic energy from the volcano propagates in the stratospheric duct. At IS22, central frequency of detected signals is close to 1 Hz.

[9] In order to get accurate estimates of the acoustic source function (time, amplitude, frequency and duration) of each explosion, a MB2000-type microbarometer has been installed 200 meters from the crater of Yasur. Signals from explosions are detected automatically using a discrete wavelet transform-based method [Mallat, 1989]. As transient signals recorded close to the crater are quite similar with a central frequency of 3–4 Hz and duration of  $\sim 1$  sec, the same wavelet is used to pick the arrival times of all signals.

[10] The main advantage of this method is its low computation time compared to the more classical STA/LTA algorithm [Withers *et al.*, 1998].

[11] Such a setting provides a unique opportunity to investigate the effects of seasonal and short-timescale atmospheric changes on the propagation, as well as to validate stratospheric wind models. For these purposes, a systematic correlation-based procedure between acoustic measurements in near field (few hundreds of meters from the main vents) and at IS22 (399 km from Yasur, back-azimuth of  $42.7^\circ$ ) has been developed. The process starts with the PMCC automatic bulletin at IS22 which provides the list of all coherent signals originating from Yasur. Time segments of five minutes, centered on the detected signals, are associated to the near field recordings after applying a time delay consistent with a stratospheric propagation. In order to improve the signal-to-noise ratio, recordings at IS22 are phase-aligned and band-pass filtered between 1 and 4 Hz. Figure 2 compares typical waveforms recorded from Yasur in the near and far field. A possible hypothesis to explain the distinct observed arrivals is their possible association to the regular

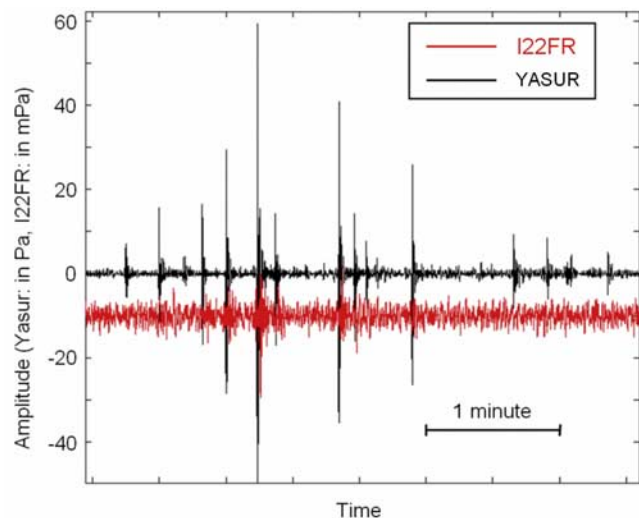


**Figure 2.** Comparison between typical measurements of infrasound from Yasur on its crater and at IS22. The time sequence at IS22 (phase-aligned signals filtered between 1 and 4 Hz) measured at the central array element is time delayed by 23 min, which corresponds to a celerity of 290 m/s. Central frequency on the crater is close to 3 Hz, and around 1 Hz when recorded in IS22.

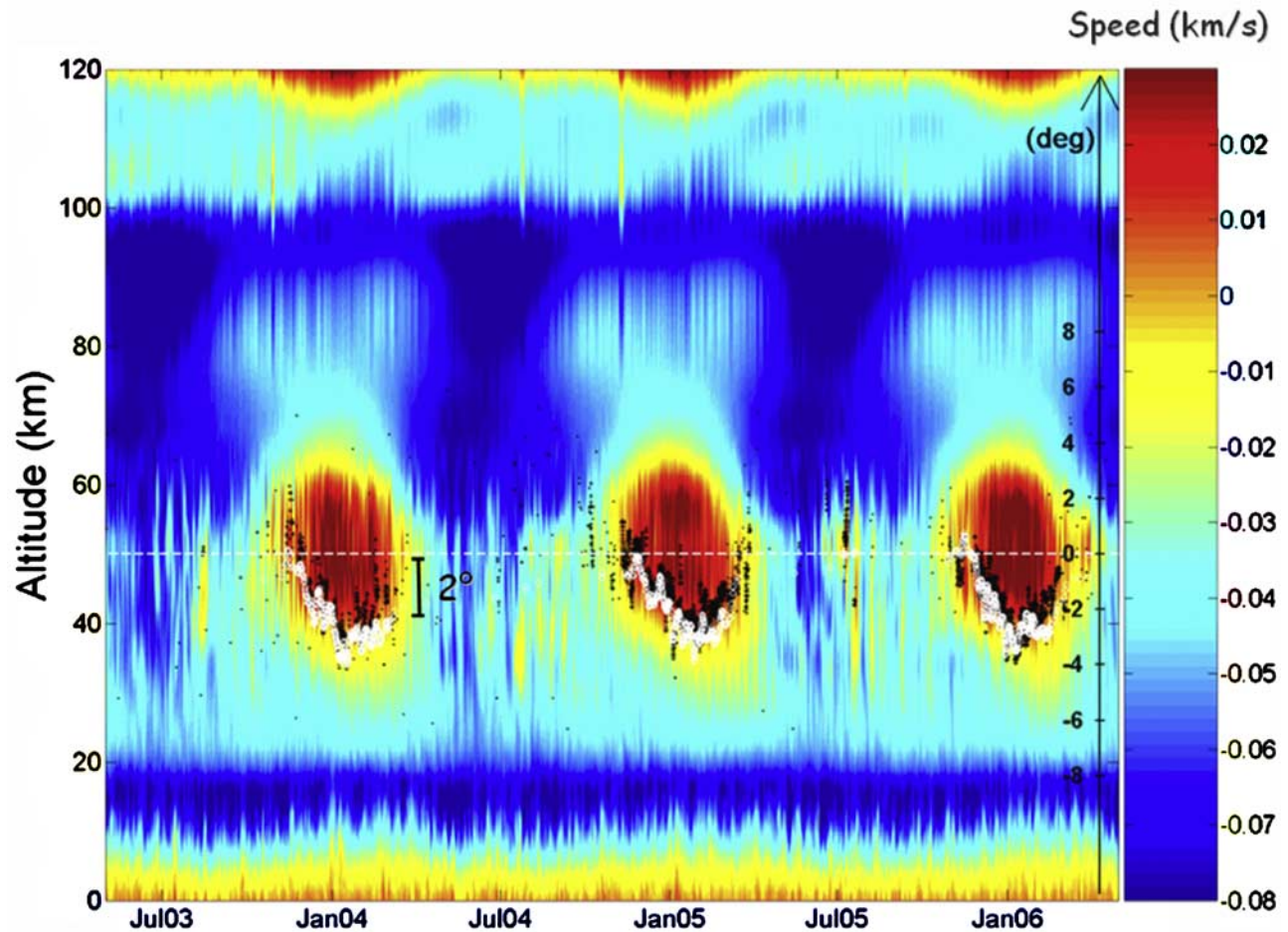


**Figure 3.** Temporal variation of the azimuthal deviation (y scale on the right) from May 2003 to May 2006, superimposed on the vertical structure of the G2S effective sound speed relative to the sound speed at the ground level (y scale on the left). Black and white dots are the PMCC and ray tracing results, respectively. The white dashed line indicates the true bearing of Yasur as seen from IS22 ( $42.7^\circ$ ). Measurements are averaged over consecutive periods of six hour length. Simulations are carried out each six hours.

breaking of over-pressurized bubbles as large as the volcanic conduit [Vergnolle and Brandeis, 1996; Hagerty *et al.*, 2000]. Traveltimes are then calculated using the cross-correlation technique. Through this procedure, the volcanic activity (number and intensity of the explosions) and celerity of the waves (horizontal propagation range divided by traveltime) are monitored throughout several years.

### 3. Validating Atmospheric Models

#### 3.1. Propagation Modeling

[12] The long range propagation is simulated using the Windy Atmospheric Sonic Propagation ray theory-based method (WASP-3D) which accounts for the spatiotemporal variations of the horizontal wind terms along the raypaths in spherical coordinates [Virieux *et al.*, 2004; Dessa *et al.*, 2005]. This method provides all needed kinematic parameters of each ray (traveltime, incidence angle, azimuthal deviation) for comparisons with measurements. With a sampling rate of 20 Hz, the expected numerical resolution at 1 Hz is of the order of  $0.5^\circ$  for the azimuth and 5 m/s for the horizontal trace velocity. These errors are significantly

smaller than the observed seasonal and short time-scale variations of the infrasound observables (section 3.2).

[13] The NRL-G2S model was run to provide a self-consistent climatological database in the Vanuatu region from May 2003 to May 2006, at 6-hours intervals [Drob *et al.*, 2003]. Following a shooting procedure, simulations were carried out with ray parameters (slowness values) derived from the measured horizontal trace velocities. The largest values ( $\sim 3$  s/km) correspond to nearly horizontal launch angles, whereas the lowest values ( $\sim 2.6$  s/km) correspond to steepest incidence angle ( $\sim 26^\circ$ ). For the simulations, 40 rays were launched with slowness values ranging from 2.6 to 3.0 s/km. Ray trajectories were calculated each day at 0, 6, 12 and 18 h UT. Only rays with bounces contained within a circle of radius 50 km around IS22 were selected. This range allows focusing on all rays reaching IS22 for comparisons with measurements. Azimuthal deviations, traveltimes and horizontal trace velocities derived from the selected rays were finally calculated by applying a weighted mean (weight linearly related to the distance separating the ray bounce to the receiver).

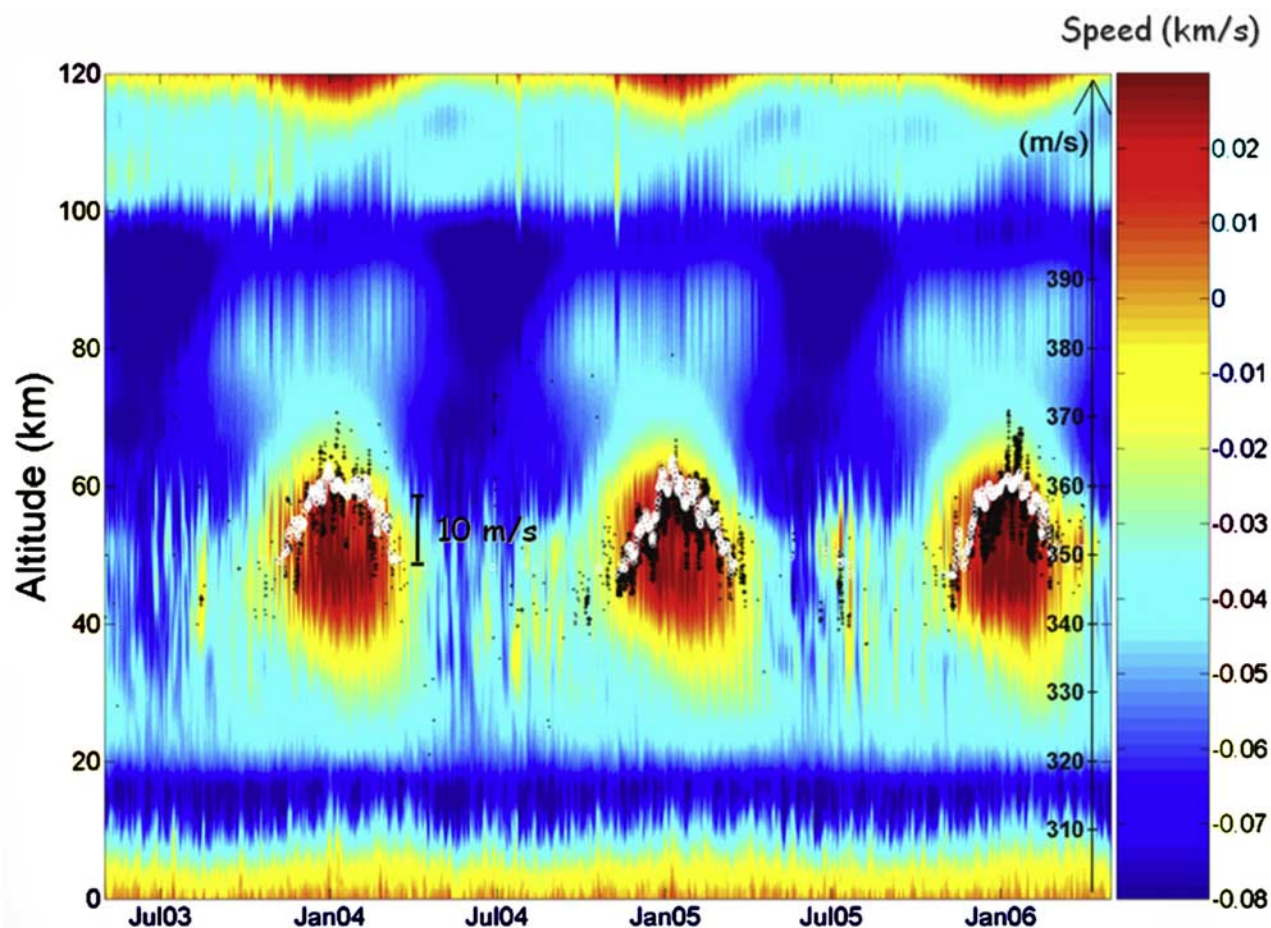


**Figure 4.** Temporal variation of the horizontal trace velocity from May 2003 to May 2006, superimposed on the vertical structure of the relative G2S effective sound speed. Black and white dots are the PMCC and ray tracing results, respectively.

### 3.2. Simulating Observations at IS22

[14] Figures 3 and 4 present the observed azimuth and horizontal trace velocity of the infrasonic waves generated by the Yasur volcano as detected at IS22. Measurements are compared to ray tracing results from May 2003 to May 2006 along with the temporal variation of the NRL-G2S effective sound speed (wind-corrected sound speed along the propagation path). During the austral summer, the prevailing westward winds allow the formation of a stratospheric waveguide below  $\sim 40$  km height. From November to March, with downwind propagation, the propagating rays reach the station after two or three bounces.

[15] Due to the seasonal variations in the strength of the transverse wind component, the apparent arrival direction of these waves does not correspond to the original launch direction. The large observed variations in the bearing of the detected signals are mainly driven by the reversibility of the zonal stratospheric wind with season. From summer to winter, the amplitude of the observed azimuthal deviation approaches  $5^\circ$  (Figure 3). From November to January, the azimuth decreases from  $43^\circ$  to  $39^\circ$  when the zonal winds are the strongest, before rising up to the true bearing ( $42.7^\circ$ ) in March when stratospheric winds reverse. The comparison between the observed and the predicted azimuths shows a similar seasonal trend. Furthermore, the simulation results

are in very good agreement with the observations even down to timescale of a few days. The errors are generally lower than  $0.5^\circ$  (less than 0.2%) for more than 90% of the time.

[16] The fluctuations of the trace velocity also present seasonal trends. In November, the wind speed in the stratosphere is not strong enough to favor stratospheric returns, thus most the rays propagate through the thermosphere where they are absorbed due to strong dissipation [Bass and Sutherland, 2004]. Only rays with shallow incidence angle (i.e., trace velocity close to the sound speed at the ground level) return back to the ground after being refracted in the stratosphere. With the reinforcement of the wind, according to the ray theory, the steepest rays are ducted in the stratospheric channel until the horizontal trace velocity becomes greater than the effective sound speed at the turning height. As a result, from November to January, as the azimuth decreases by  $\sim 4^\circ$ , an increase of  $\sim 15$  m/s of the trace velocity is noted. As for the azimuthal deviation, the seasonal fluctuations of the trace velocity are well predicted by the NRL-G2S specifications, the largest biases remaining in the order of 5 m/s.

[17] Figure 5 compares the predicted celerity to the measured one from July 2004 to July 2005 following the procedure described in section 2. As opposed to the devia-

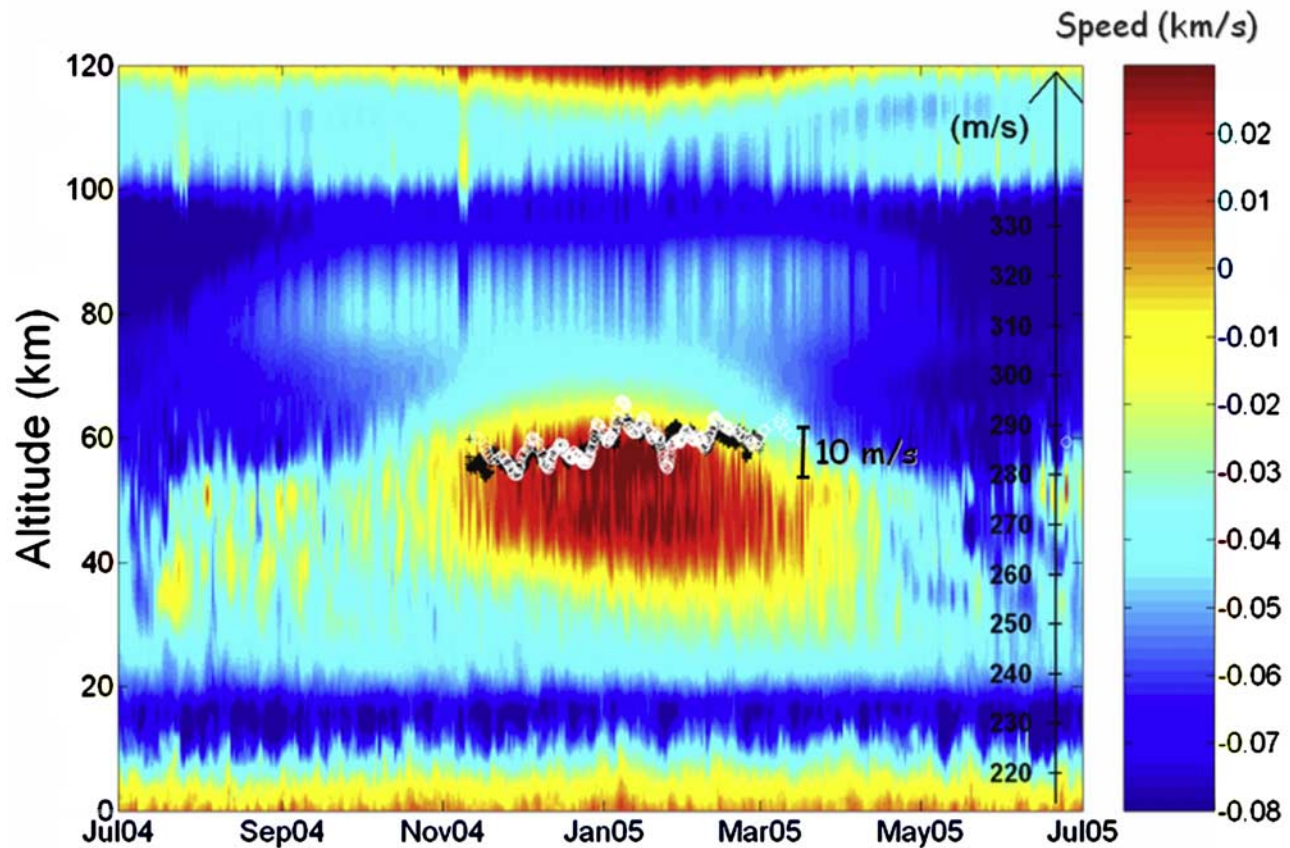


**Figure 5.** Temporal variation of the celerity from July 2004 to July 2005, superimposed on the vertical structure of the G2S relative effective sound speed. Black and white dots are the PMCC and ray tracing results, respectively.

tions of the azimuth and trace velocity, there is no clear seasonal variation of the celerity. The celerity ranges from 280 to 290 m/s, which are typical values characterizing the propagation of stratospheric waves [Brown *et al.*, 2002]. Deviations of 5–10 m/s are observed down to a timescale of few weeks. They are associated to modulations of the general circulation in the stratosphere. In our region of interest, zonal wind reversals often result from significant quasi-stationary subtropical disturbances that formed in connection with large stationary ridges in the polar winter stratospheric wind jet [Le Pichon *et al.*, 2005a]. Again, simulations and observations are in very good agreement with maximum errors lower than 5 m/s.

#### 4. Concluding Remarks

[18] Recent case studies dealing with infrasound propagation from ground-truth events demonstrated the accuracy of the semiempirical NRL-G2S atmospheric model from the ground up to 55 km [Olson *et al.*, 2006; Ceranna and Le Pichon, 2006]. For the first time to our knowledge, the NRL-G2S semiempirical model has been validated consistently in the Vanuatu region up to the stratosphere, through a multiyear monitoring of infrasound. From May 2003 to May 2006, ~90 000 transient signals associated to the breaking of over-pressurized bubbles at the top of the volcanic conduit of Yasur have been detected by the IS22

station and automatically associated with nearby measurements. Our simulation results provide a very good description of the general seasonal changes as well as short-timescale fluctuations of the measurements. The errors are generally lower than  $0.5^\circ$  for the azimuth deviation, and 5 m/s for the trace velocity and the celerity. For large propagation range, most of the energy propagates in the stratospheric duct due to very weak attenuation. Thus one can expect that the use of appropriate propagation tools along with the NRL-G2S specifications would provide accurate enough simulations for most of the infrasound observations in the 0.5 to 4 Hz band.

[19] More studies like the one presented here will better determine the role of different factors that influence propagation predictions and could estimate more precisely how large the errors in the upper wind models are. Continuing investigations into infrasonic signals from active volcanoes will certainly improve our understanding of the atmosphere and help advance the development of automated source location procedures for operational infrasound monitoring.

[20] **Acknowledgments.** The authors are grateful to M. Garcés for his interest in this study and for the helpful discussions we had during the completion of this work. We would like also to thank the NASA Goddard Space Flight Center, Global Modeling and Assimilation Office (GSFC-GMAO), and the NOAA National Centers for Environmental Prediction (NCEP) for providing data that went into the NRL-G2S atmospheric specifications. Support was also provided by Institut de Physique du Globe de Paris, Coordination de la Recherche Volcanologique and Ministère de

l'Écologie et Développement Durable to install instruments close to the Yasur volcano. The authors also appreciate the valuable comments of P. Gaillard, J. Vergoz, P. Mialle, and E. Nayman, which helped to improve the manuscript.

## References

- Bass, H. E., and L. C. Sutherland (2004), Atmospheric absorption in the atmosphere up to 160 km, *J. Acoust. Soc. Am.*, *115*, 1012–1032.
- Brown, D. J., C. N. Katz, R. Le Bras, M. P. Flanagan, J. Wang, and A. K. Gault (2002), Infrasonic signal detection and source location at the Prototype Data Centre, *Pure Appl. Geophys.*, *159*, 1081–1125.
- Bush, G. A., Y. A. Ivanov, S. N. Kulichkov, A. V. Kuchayev, and M. V. Pedanov (1989), Acoustic sounding of the fine structure of the upper atmosphere, *Izv. Acad. Sci. USSR Atmos. Oceanic Phys.*, Engl. Transl., *25*, 251–256.
- Cansi, Y. (1995), An automatic seismic event processing for detection and location: The PMCC method, *Geophys. Res. Lett.*, *22*, 1021–1024.
- Ceranna, L., and A. Le Pichon (2006), The Buncefield explosion: A benchmark for infrasound monitoring in Europe, paper presented at 2006 Infrasound Technical Workshop, Geophys. Inst., Univ. of Alaska Fairbanks, Fairbanks, Alaska. (Available at <http://www.gi.alaska.edu/infrasound/IT2006/>)
- Delclos, C., E. Blanc, P. Broche, F. Glangeaud, and J. L. Lacoume (1990), Processing and interpretation of microbarograph signals generated by the explosion of Mount St. Helens, *J. Geophys. Res.*, *95*, 5485–5494.
- Dessa, J.-X., J. Virieux, and S. Lambotte (2005), Infrasound modeling in a spherical heterogeneous atmosphere, *Geophys. Res. Lett.*, *32*, L12808, doi:10.1029/2005GL022867.
- Donn, W. L., and N. K. Balachandran (1981), Mount St. Helens eruption of 18 May 1980: Air wave and explosive yield, *Science*, *213*, 539–541.
- Donn, W. L., and D. Rind (1971), Natural infrasound as an atmospheric probe, *Geophys. J. R. Astron. Soc.*, *26*, 111–133.
- Drob, D. P., J. M. Picone, and M. Garcés (2003), Global morphology of infrasound propagation, *J. Geophys. Res.*, *108*(D21), 4680, doi:10.1029/2002JD003307.
- Garcés, M., M. Willis, C. Hetzer, A. Le Pichon, and D. Drob (2004), On using ocean swells for continuous infrasonic measurements of winds and temperature in the lower, middle, and upper atmosphere, *Geophys. Res. Lett.*, *31*, L19304, doi:10.1029/2004GL020696.
- Hagerty, M. T., S. Y. Schwartz, M. A. Garcés, and M. Protti (2000), Analysis of seismic and acoustic observations at Arenal Volcano, Costa Rica, 1995–1997, *J. Volcanol. Geotherm. Res.*, *101*, 27–65.
- Hedlin, M., M. A. Garcés, H. Bass, C. Hayward, G. Herrin, J. Olson, and C. Wilson (2002), Listening to the secret sounds of Earth's atmosphere, *Eos Trans. AGU*, *83*, 564–565.
- Kulichkov, S. N., K. V. Avilov, O. E. Popov, A. I. Otrezov, G. A. Bush, and A. K. Baryshnikov (2004), Some results of simulation of long-range infrasonic propagation in the atmosphere, *Izv. Russ. Acad. Sci. Atmos. Oceanic Phys.*, Engl. Transl., *40*, 202–215.
- Lardy, M., R. Priam, and D. Charley (1999), Lopévi: Résumé de l'activité historique et de l'activité récente, *LAVE Tech. Rep.* *77*, 5 pp., Off. de la Rech. Sci. et Tech. Outre-Mer, Nouméa, New Caledonia.
- Le Pichon, A., E. Blanc, D. Drob, S. Lambotte, J. X. Dessa, M. Lardy, P. Bani, and S. Vergnolle (2005a), Infrasound monitoring of volcanoes to probe high-altitude winds, *J. Geophys. Res.*, *110*, D13106, doi:10.1029/2004JD005587.
- Le Pichon, A., E. Blanc, and D. Drob (2005b), Probing high-altitude winds using infrasound, *J. Geophys. Res.*, *110*, D20104, doi:10.1029/2005JD006020.
- Liszka, L., and M. A. Garcés (2002), Infrasonic observations of the Hekla eruption of February 26, 2000, *J. Low Frequency Noise Vibration Active Control*, *21*(1), 1–8.
- Mallat, S. (1989), A theory for multiresolution signal decomposition: The wavelet representation, *IEEE Trans. Pattern Anal. Mach. Intel.*, *11*, 674–693.
- McClelland, L., T. Simkin, M. Summers, E. Nielsen, and T. C. Stein (1989), *Global Volcanism: 1975–1985*, 655 pp., Prentice-Hall, Englewood Cliffs, N. J.
- Olson, J. V., C. R. Wilson, S. McNutt, and G. Tytgat (2006), Infrasonic wave observations of the January 2006 Augustine Volcano eruptions, *Eos Trans. AGU*, *87*(52), Fall Meet. Suppl., Abstract V51C-1685.
- Reed, J. W. (1987), Air pressure waves from Mount St. Helens eruptions, *J. Geophys. Res.*, *92*, 11,979–11,992.
- Rind, D. (1978), Investigation of the lower thermosphere results of ten years of continuous observations with natural infrasound, *J. Atmos. Terr. Phys.*, *40*, 1199–1209.
- Ripepe, M., P. Poggi, T. Braun, and E. Gordeev (1996), Infrasonic waves and volcanic tremor at Stromboli, *Geophys. Res. Lett.*, *23*, 181–184.
- Robin, C., and M. Monzier (1994), Volcanics hazards in Vanuatu, *Tech. Rep.* *16*, 15 pp., Geol. and Geophys., Off. de la Rech. Sci. et Tech. Outre-Mer, Nouméa, New Caledonia.
- Vergnolle, S., and G. Brandeis (1996), Strombolian explosions: A large bubble breaking at the surface of a lava column as a source of sound, *J. Geophys. Res.*, *101*, 433–448.
- Virieux, J., N. Garnier, E. Blanc, and J.-X. Dessa (2004), Paraxial ray tracing for atmospheric wave propagation, *Geophys. Res. Lett.*, *31*, L20106, doi:10.1029/2004GL020514.
- Wilson, C. R., and R. B. Forbes (1969), Infrasonic waves from Alaskan volcanic eruption, *J. Geophys. Res.*, *74*, 4511–4522.
- Wilson, C. R., J. V. Olson, C. Szuberla, S. McNutt, G. Tytgat, and D. Drob (2006), Infrasonic array observations at I53US of the 2006 Augustine volcano eruptions, *News. 13*, Inframatics, Scripps Inst. of Oceanogr., Univ. of Calif., San Diego, San Diego. (Available at <http://www.inframatics.org>)
- Withers, M., R. Aster, C. Young, J. Beiriger, M. Harris, S. Moore, and J. Trujillo (1998), A comparison of select trigger algorithms for automated global seismic phase and event detection, *Bull. Seismol. Soc. Am.*, *88*, 95–106.

K. Antier and A. Le Pichon, CEA/DASE/LDG, BP12, F-91680 Bruyères-le-Châtel, France. (alexis.le-pichon@cea.fr)  
 M. Lardy, IRD Center, BPA5, 98848 Nouméa Cedex, New Caledonia.  
 S. Vergnolle and C. Zielinski, LDSG-IPGP, 4 Place Jussieu, F-75252 Paris Cedex 05, France.